Direct Bubble Size Measurement in a Mechanical Flotation Cell by Image Analysis and Laser Diffraction Technique - A Comparative Study

Mazahernasab, Reyhane; Ahamadi, Rahman*[+]; Ravanasa, Elmira

Department of Mining Engineering, Imam Khomeini International University (IKIU), Qazvin, I.R. IRAN

ABSTRACT: *In this study, a comparative measurement of bubble sizes in a two-phased medium (water and air) was performed in a mechanical flotation cell by Image Analysis (IA) and Laser Diffraction (LD) methods. The bubbles were generated in a mechanical cell with dimensions of 25*15*17 cm^3. To determine the bubbles' size by the LD method, the bubbles were transferred from the cell to the Laser Particle Size Analyzer (LPSA) device through a hole in the cell, and $D_b(50)$ of bubbles were also calculated from their scattering pattern data. A bubble viewer, made of Plexiglass with certain dimensions, including two main parts (sampling tube and viewing chamber) was employed for the IA method. Comparative experiments were conducted in the different conditions affecting the bubble sizes, which are the impeller speed, solution temperature, pH value, and frother types. Results indicated that the two measurement methods were in good agreement while bubbles' sizes were in a range of +400-800 microns. The difference between LD and IA results was less than 7% in the range of +400-800. In the size range of -200 microns, LD and IA results difference increased to 36%. Moreover, in all experiments with the same conditions, the size of the bubbles by the LD method was recorded smaller than that by the IA method. Considering the fact that bubbles in the mechanical flotation cell are usually in the size range of +600 -2000 microns, and in this range, LD and IA results had a negligible disagreement, LD can be successfully employed for the bubble size measurement in mechanical flotation cells.*

KEYWORDS: *Bubble size distribution; Mechanical flotation; Laser Diffraction Technique (LDT); Image Analysis Technique (IAT); Bubble size measurement.*

INTRODUCTION

Air bubbles play a significant role in the flotation system, as they carry hydrophobic particles up to the surface, transfer them to the froth phase, and generally separate them from hydrophilic particles. In this regard, bubbles should have an appropriate size distribution, and there should be a remarkable correlation between the particle and the bubble size distribution [1, 2]. The rate of mineral recovery is heavily dependent on the bubble size distribution in the flotation process [3]. In a study by *Ahmed* and *Jamson* [3], they reported that by the bubble size reduction from 655 to 75 micron, the rate of quartz flotation increases almost one hundred-fold [4].

***** *To whom correspondence should be addressed.*
+ *E-mail*: *Ra.ahmadi@eng.ikiu.ac.ir*
1021-9986/2021/5/1653-1664 *11/$/6.01*

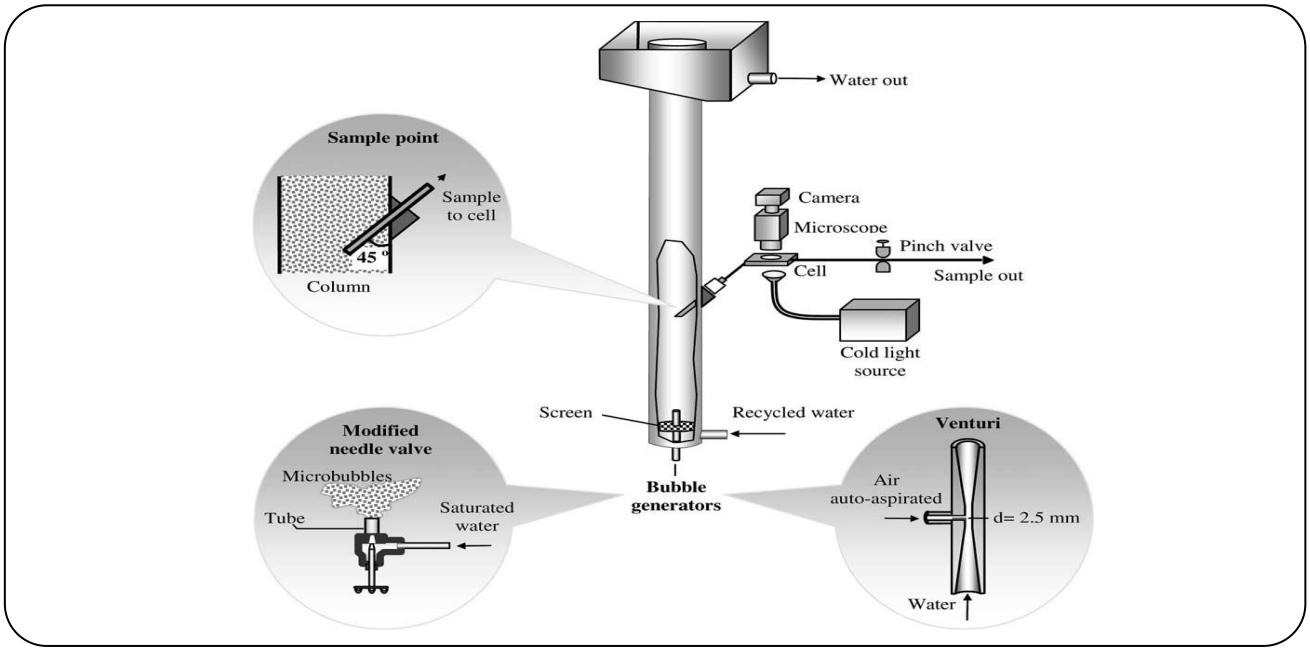

Fig. 1: The LTM-B sizer system [15].

Also, there has been a linear relationship between the first-rate constant and the bubble surface area flux recording by *Gorain et al.* [5]. They concluded that the bubble surface area flux as a function of gas dispersion, which is proportional to the superficial gas velocity and inversely proportional to the Sauter mean bubble diameter, can be used as a single, scaleable parameter to affect the rate of flotation recovery [5]. All of these studies clearly determine the importance of bubble size distribution knowledge so as to predict cell performance.

Thus, bubble size measurement has considerable importance to control a flotation process. Several techniques have been used to determine the bubbles' size [6,7], generated in the flotation, especially X-ray [8], empirical and semi-empirical relations based on flow dynamics "Stokes law" [9], electrical-resistance measurement [10], and ultrasound methods [11]. These methods are sophisticated, time-consuming, less accurate, and indirect. In these methods, first, bubbles are produced outside of a mechanical flotation cell, then the bubble size is measured, and fed into the flotation cell, and, by doing so, the deviation would be shown from the actual bubbles' size which was produced into a cell. The information which is derived from these methods makes several errors.

The image analysis method has been applied by many researchers to determine the bubble and micro-bubble size distribution. *Ksentini et al.* [12] used the method of video recording and image treatment to determine oxygen micro-bubble diameter, their rising speed, and gas hold-up in an electro-flotation column. Also, *Nesset et al.* [13] employed the image analysis method to measure the bubble size in mechanical flotation cells. *Hernandez-Aguilar* [14] presented a bubble sampler that includes a viewing chamber and a sampler tube. This simple design as well as proper backlighting, produced photos with high contrast. The quality of the photos was enough to be automatically processed. This bubble sampler that was developed at McGill University for the first time, was named MBSA. LTM-B sizer, as shown in Fig. 1) is a novel method to measure the bubble size. This method is a combination of digital and microscopic image analysis [15]. In this method, bubbles enter a viewing chamber through a column, and after a reduction in their speed, they are photographed.

Although, Unlike indirect measuring systems, Image Analysis (IA) which is a typical direct method for bubble size measurement inside flotation cells, creates also some challenges. The main challenge is the variation of the distance between bubbles and the lens focal plane due to the spiral motion of bubbles in the shooting zone of mechanical cells [14]. Moreover, differences in optical conditions (i.e. light, temperature, etc), bubbles overlap, blurring of some bubbles in images, bubbles aggregation,

and a relatively time-consuming process of measurement in other trials may lead to errors in the IA method.

The Laser Diffraction (LD) technique has been used to measure the size of dry solid particles, colloids, and emulsions since the mid-70s. LD is applied by a Laser Particle Size Analyzer (LPSA) to measure the size of particles/bubbles in an aqueous or aerial environment. This technique is determined as a non-destructive and the non-intrusive method which relies on the fact that the laser diffraction angle is inversely proportional to particle size [16]. LD is applicable for particle size range from 0.1 µm to 3000 µm according to ISO13320-1 [17]. In 2004, LD was developed to measure the size distribution of colloidal aprons gas (A type of foam, which is used in the separation process) [18]. Afterward, it was applied to determine the size distribution of fine bubbles in the range of micrometer and nanometer. *Hudson et.al* [19] measured the bubble size distribution in dissolved air flotation by the LD method and confirmed that this method is capable of being used for industrial operations since it is a time-saving technique and easy to repeat.

As LD is a direct measuring technique, it has not been applied to measure the size of bubbles into a mechanical flotation cell, and its results have not been compared with IA method results, which is a direct measurement method thus far. Hence, this study is going to present a new step-up for the measurement of bubble size distribution, which is produced in a floatation cell, using the LD method. To validate the accuracy of the newly presented set-up and to compare, LD and IA methods were simultaneously used to measure the bubble size distribution. Their results were compared qualitatively and quantitatively. The results of this investigation can be used to control the flotation separation systems more precisely.

EXPERIMENTAL SECTION

Materials

Bubbles were generated in a mechanical flotation cell of 17×15×25 cm^3. In tests, two typical flotation frothers were used separately in experiments: methyl isobutyl carbinol (MIBC) with the molecular weight of 102.17 g/mol (manufactured by Sigma Aldrich Company, USA) and polypropylene glycol (A65) with the molecular weight of 395.61 g/mol (manufactured by Cyanamide Company, USA). To generate bubbles, a certain amount of frother (30 ppm) was added to the twice-distilled water in the cell. After adjusting the pH and temperature, the air valve was opened at the rate of 0.5 L/min, and bubbles began to produce. Bubbles were continuously transferred to the LPSA, using different pressures. For pH adjustment, sulfuric acid (H_2SO_4) of 98% and sodium carbonate (Na_2CO_3, supplied from the Merck Corporation, Germany.) The pH value was measured by a pH meter model MP230, Switzerland. In all experiments, twice-distilled water was used for preparing the aqueous solutions.

Laser diffraction (LD)

The LPSA "MS2000", manufactured by Malvern Co., was employed to determine the bubble size distribution. To transfer the bubbles from the flotation cell to LPSA, a hole was created on the body of the cell (Figs. 2 and 3). The hole was located 2 cm above the bottom of the cell, and a tube linked it to the LPSA to facilitate transferring the bubbles from the cell toward the LPSA. The flotation cell was placed at the closest possible distance from LPSA (15cm) to reduce the bubble collapse. The Mie optical model was selected in the LPSA to calculate the bubble size distribution. Measurements were performed every four seconds, while the light reflection index was 1.00 and 1.33 for water and bubble, respectively. Various parameters (frother types, aeration rate, temperature, pH, and impeller speed), which are effective on the size of bubbles, were examined to assess the LD ability for the bubble size distribution. To increase the accuracy of the results, each measurement was repeated four times and the median bubble diameter was calculated on a volumetric basis. The average of four measurements was shown as $D_b(50)$ which represents the size of the bubble at which there is 50% of the distribution. The coefficient of variation of results obtained 1.64%, which is acceptable according to BS ISO 13320-1[17]. Moreover, the weighted residual values of tests, which represent the fit of the calculated data obtained by the model with the measured data, were in the range of 0.46 -0.75%. The weighted residual value less than 1% indicates a good and acceptable fit and greater than 1% indicates the wrong choice of refractive index values.

The laser diffraction method is based on the relationship between the light scattering pattern and the particle size [20]. In this method, light scattering by particles is recorded by detectors and is converted to bubble size distribution by mathematical equations. The spatial distribution of light scattering is called

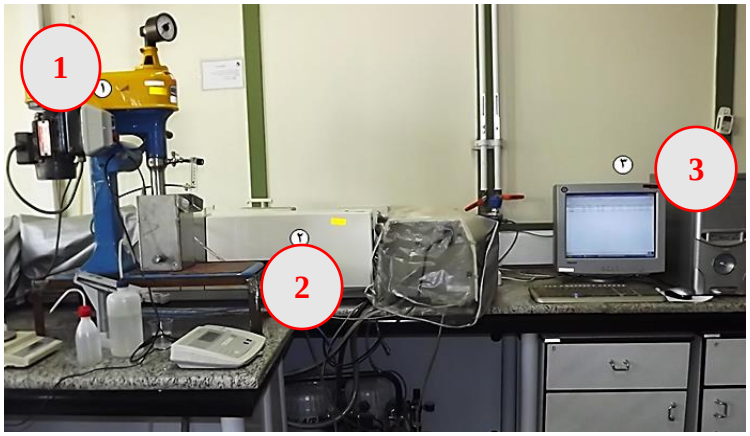

Fig. 2: Laser Diffraction system components. 1) Flotation machine, 2) LPSA -Laser Particle Size Analyzer, and 3) Computer system.

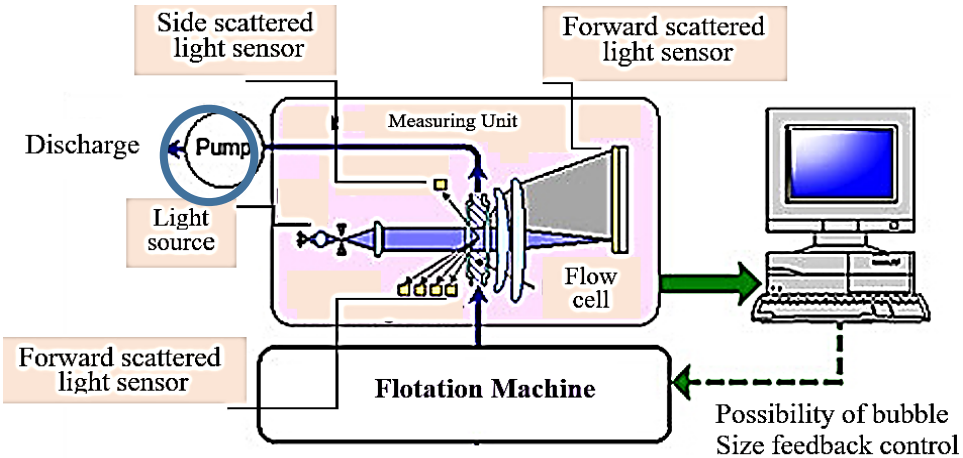

Fig. 3. Internal components of the bubble size measurement by LD method[20].

the scattering pattern. This pattern is measured by detectors and is converted to the size distribution of particles by proper optical models. The scattering pattern created by each particle is an indication of the particle's dimensions, which is transformed into an accurate and repeatable image of the dimensional distribution by mathematical methods. Fig. 4 shows a scattering pattern of a particle with a diameter of 5 microns.

The diffraction pattern depends on the ratio of particle diameter to wavelength. Therefore, this pattern changes not only with the particle size but also with the wavelength. Scattering pattern depends on the shape and the optical properties of particles too [20].

Five tests were selected from the different conditions to examine the accuracy of LD bubble size measurement in comparison with the image analysis results. A bubble viewer,

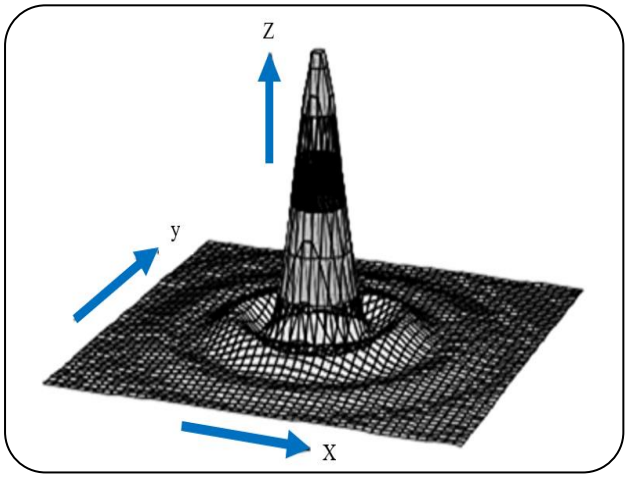

Fig. 4: Scattering pattern of a particle with a diameter of 5 microns. X: X-axis detector, Y: Y-axis detector, Z: relative intensity [20].

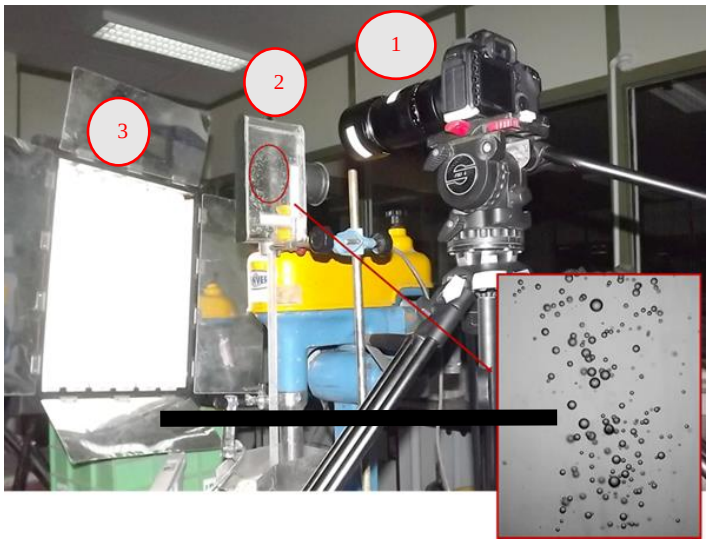

Fig. 5: Image analysis system components. 1) Digital Camera, 2) Light source, 3) Bubble Viewer.

made of Plexiglas with certain dimensions, including two main parts (sampling tube and viewing chamber) was employed for IA. Fig. 5 shows the measurement equipment of the image analysis system in a mechanical flotation cell.

Before imaging, the bubble viewer was filled with the combination of water and frother, with the same frother concentration, pH, and temperature as the flotation cell in order not to change the bubbles environment during transferring from flotation cell to bubble viewer. Then, a bubble viewer sampling tube was inserted gently into the cell at an angle of 90 ° to the ground. Bubbles were going up from the sampling tube and were photographed when reached the chamber. A source of cold light (LED) was placed behind the bubble viewer at the angle of 90° to the ground.

The 15° slope of the chamber lets the bubbles move almost as a single layer near the viewing chamber screen. This slope would have minimized the overlapping of the bubbles in the photos. Photos were taken by a digital camera "Canon 5D Mark ΙΙ" with a microlens. The measurement scale was placed exactly at the focal plane. The sharp and clear bubbles were carefully chosen for the processing step, where the blurry bubbles could not be considered. The cold light source was perpendicular to the rear panel. To increase the accuracy of the measurements, at least 200 images were taken in each test and were randomly used for the processing step. "Projected area diameter" was determined by an image analyzer software. Then, the $D_b(50)$ and the size distributions of bubbles were calculated.

RESULTS AND DISCUSSION

LD bubble size measurement

Frother type

Frothers have a multi-polar structure. Through flotation, froth is adsorbed at the liquid/gas interface, and it forms a liquid film on the bubble surface and improves bubble sustainability [21]. MIBC and A65 are two typical frothers in the flotation separation. The main difference between bubbles produced with the MIBC and A65 is attributed to the molecular structure of these two frothers, which influences the formation of a hydrogen bond with water molecules [21- 24]. Hydrophilic-Lipophilic Balance (HLB) is one of the most common indicators evaluating the froth-ability of a frother [22]. HLB relies on the functional groups in the formula of frothers. HLB value for MIBC and A65 is 6.05 and 8.69, respectively [25]. *Nesset et al.* [26] suggested that the minimum diameter of bubbles lowered by increasing HLB. Frothers with higher HLB values are more hydrophilic, which means they are more soluble in water, thereby having more hydrophilic groups and forming hydrogen bonds with water [25, 27,28].

A65, has a higher molecular weight, subjects to generate viscous and stable bubbles. MIBC owns only one hydroxyl group and creates an angled layer of molecules on the bubble surface, while A65 has several oxygen units that form hydrogen bonds with water and result in molecules

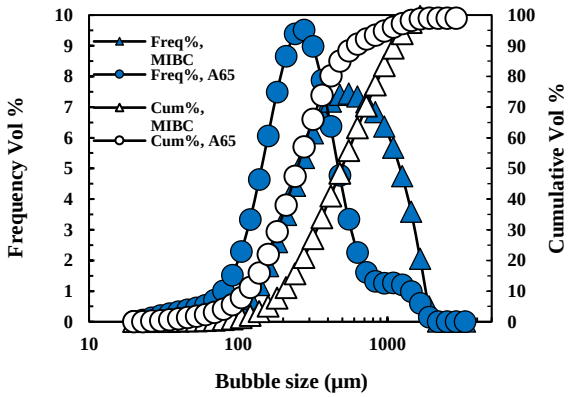

Fig. 6: The effect of frother type on bubble size distribution

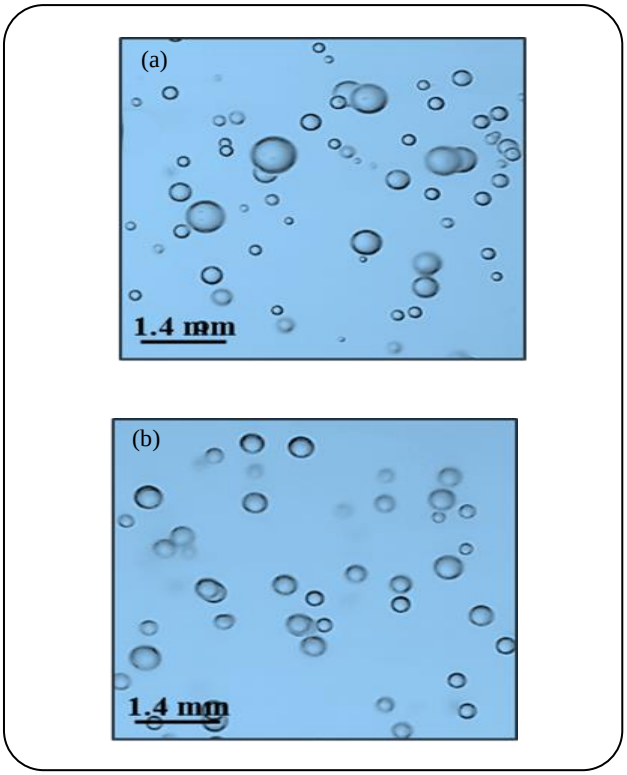

Fig. 7: The image of bubbles in the presence of frothers a) MIBC b) A65

that lie in the bubble surface [29]. The contact between bubbles and water molecules decreases the coalescence of bubbles. As a consequence, in the presence of A65, smaller bubbles would be generated.

To investigate the effect of frother type on the bubble size, experiments were conducted, while other parameters were kept at constant values: pH 7, temperature 27 ^{o}C, impeller speed 1050 rpm. Bubble size measurement in the presence of the two different frothers indicated that D_b (50) of bubbles were generated in the presence of A65 and MIBC are 314 and 438 µm, respectively (Fig. 6). Smaller bubbles by A65 frother in comparison with MIBC have been reported in various investigations [30]. LD measurements showed that the distribution width of bubble size in the presence of MIBC is higher than that in the presence of A65. These results were confirmed by the IA which showed the bubble size variations in the presence of these two frothers (Fig. 7).

pH

It is well-documented that bubbles are smaller and stabler as pH is increased [31, 32, 33]. To check the ability of LD for the measurement of bubble size distribution in various pHs, MIBC was utilized as the frother, the temperature was adjusted at 27 ^{o}C, impeller speed was set to 1050 rpm and three different pH values were examined: 5, 9, and 11. LD results demonstrated (Fig. 8) that by increasing the pH values, D_b(50) is reduced from 427 to 388 µm. Furthermore, the curve of bubble size distribution shifted to the left by increasing the pH. Fig. 9 shows image analysis results. It illustrates bubble size reduction with increasing pH. Moreover, bubble aggregation can be observed at low pH values (Fig. 9).

According to *Jin et al.* [34], an increase in OH^- concentration has two opposite effects: 1) It increases the surface charge of the bubbles and helps them remain stable and small by electrostatic repulsion. 2) It also increases the ionic strength of the solution and eliminates the effective repulsive force between the bubbles and accumulates the bubbles. According to Jin, the former effect is dominant, and at higher pH values, the bubbles are finer and more stable. Moreover, based on researches, by increasing the pH or the concentration of OH- ions in the water, the sheer amount of bubble zeta potential increases, and the surface charge of the bubbles becomes highly negative. As a result of the increased bubble zeta potential, the surface repulsion force prevents the bubbles from approaching each other, and, thus their coalescence and enlargement [35].

Temperature

The effect of temperature on the bubble size distribution has been investigated for various aspects such as the impact of gas solubility in water and gas viscosity [36-38]. *Wu et al.[*33] suggested that temperature was important for the solubility of gases in water, and, also,

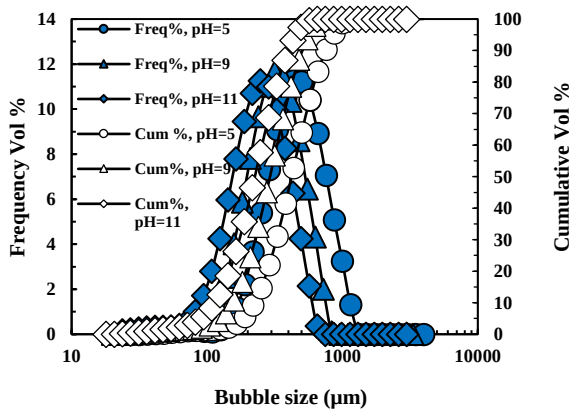

Fig. 8: The effect of pH on bubble size distribution.

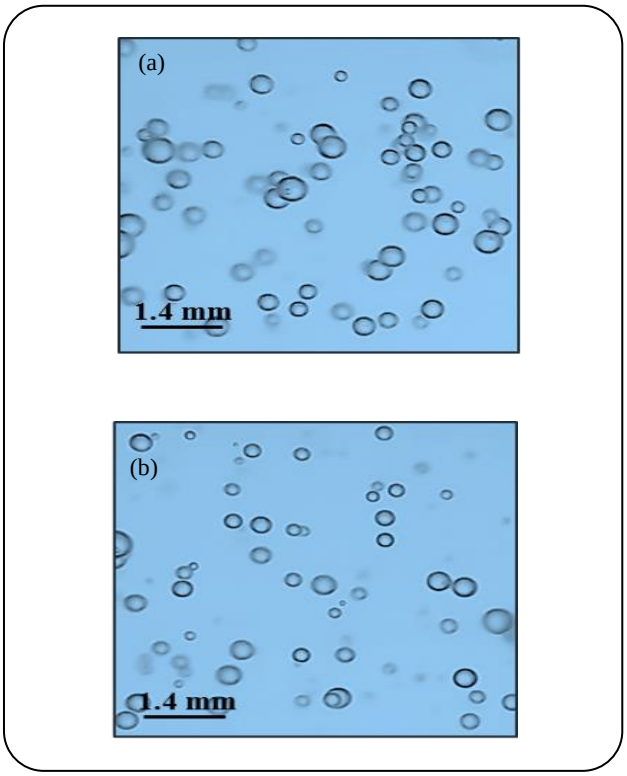

Fig. 9: The image of bubbles at different pH a) 5, b) 11.

for the coalescence of bubbles. They indicated that bubble diameter increased as the temperature increased from 50 to 72 ºC. *Ahmadi* [39] proved that an increase in temperature from 14 to 40 °C resulted in an increase in $D_b(50)$ from 135 nm to 52000 nm. This phenomenon can be due to the effect of temperature on the dissolution of gases in water. *Zhang et al.* [40] demonstrated that as the temperature increased from 28 to 42 °C, the size of bubbles increased and at 37 °C they reached their maximum size and, then, declined. The authors mentioned that reducing gas dissolution in water was the reason for increasing bubble size and declared that the dissolution of gas would get its minimum at 37 °C.

To examine bubble size changes at different temperatures, MIBC was used as a frother, pH was kept at 7, and impeller speed was set to 1050 rpm. Results of the bubble size measurement by LD (Fig. 10) exhibits that increasing the temperature from 4 to 46ºC leads to an increase in $D_b(50)$ from 327 to 1000 µm. Moreover, the curve of bubble size distribution shifted to the right when the temperature raised. Increasing the bubble size has been confirmed by IA by raising the temperature (Fig. 11).

Preval et al. [41] studied effective parameters on the bubble size distribution and found that viscosity has two main effects on the bubble size: 1) higher viscosity increases the probability of bursting larger bubbles into smaller bubbles due to increased viscous forces on the bubble. It also delays the bubble coalescence by delaying fluid film drainage in the liquid/gas interface. 2) Weber's number increases with the increase of viscosity, and, as a result, the liquid phase breakage becomes more difficult to produce bubbles. The results of this study showed that the bubble diameters are more influenced by the former effect, and by increasing the viscosity, larger bubbles break into smaller ones.

Impeller speed

Various investigations indicated that the bubble size distribution can decrease by increasing the impeller speed [42, 43, 44]. The size of bubbles in a flotation system is a function of three hydrodynamic processes, including bubble production in the gas generator, bubble breakage, and bubble coalescence [45, 46]. The last two mechanisms are controlled by the turbulent environment, which is restrained by the impeller speed [43]. The role of the impeller is dissolving air into the water to produce bubbles, and, thus, more air is dispersed in the water when the impeller spines faster. Subsequently, the bubble breakage at higher impeller speeds leads to a smaller bubble size [44, 47].

To investigate the effect of impeller speed on the bubble size distribution, MIBC was used as a frother, pH value was set at 7, and the temperature was adjusted at 27 ^{0} C. LD results (Fig. 12) show that the bubble size distribution shifted to the finer sizes and the $D_b(50)$ decreased from 727 to 284 µm by raising the impeller speed from 700 to 1200 rpm. The Image of bubbles at

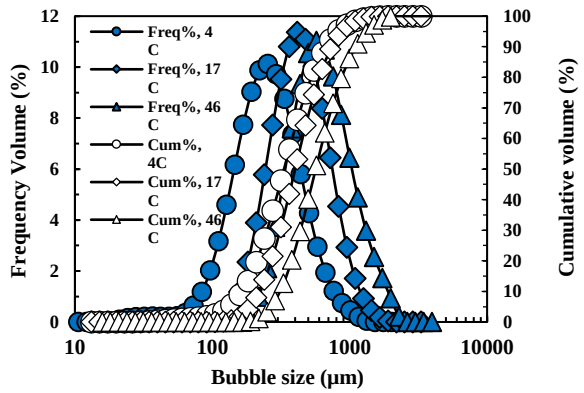

Fig. 10: The effect of temperature on bubble size distribution.

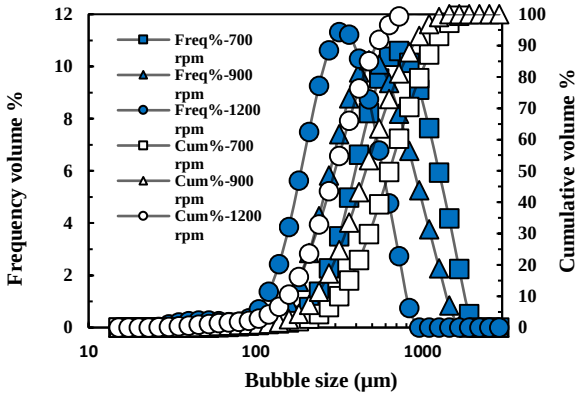

Fig. 12: The effect of impeller speed on bubble size distribution at an aeration rate of 0.5 lit/min and MIBC concentration of 30 ppm.

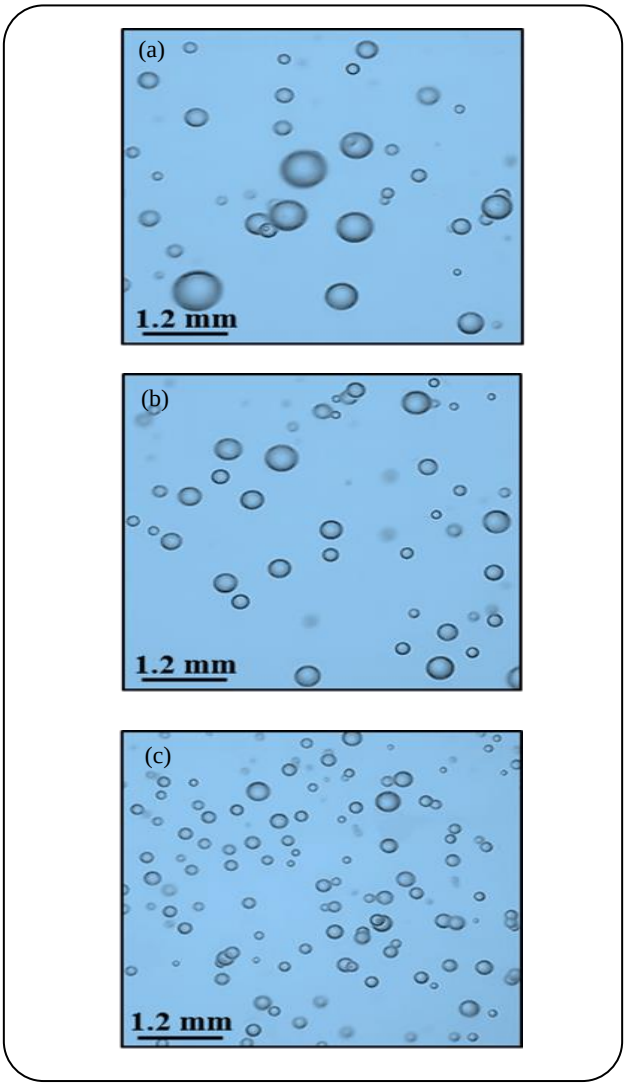

Fig. 11: The image of bubbles at different Temperatures a) 46, b) 17, c) 4 °C.

different impeller speeds confirmed the LD measurements (Fig. 13). The smallest bubbles were generated when the impeller speed was at the highest power (1200 rpm) which means that finer-size bubbles were produced at high impeller speeds.

Gorain et al. [48] presented the following empirical model through the information obtained from extensive experiments, using three types of impellers in a flotation cell of 3 m^3 in Tasmania and Western Australia:

$$S_b = 123 N_s^{0.44} \left(\frac{Q}{A}\right)^{0.75} A_s^{-0.10} P_{80}^{-0.42} \quad (1)$$

$$d_{32} = \frac{6 J_g}{S_b} \quad (2)$$

Where N_s is peripheral impeller speed (m/s), $\frac{Q}{A}$ is the aeration rate per unit section area of the cell (cm/s), A_s is the aspect ratio of the impeller, P_{80} is the size of 80% passed of feed (microns), S_b is Bubble surface flux, J_g is the superficial gas velocity (cm/s) and d_{32} is bubble Sauter mean (microns). According to Gorain's model as the impeller speed increases, the bubble's Sauter means diameter decreases. It seems that in higher impeller speeds bubble breakage leads to smaller bubbles. *Grau* [49] also agreed that with increasing the impeller speed, the number of fine bubbles increases. The role of impeller speed on reducing bubble size seems to be related to the bursting of large bubbles into smaller ones at higher speeds.

Table 1: A comparison between the results of bubble size measurements using LD and IA methods.

Impeller speed (rpm)	Temperature (°C)	pH	Frother	$D_b(50)$ IA (µm)	$D_b(50)$ LD (µm)	$\frac{D_b(50)IA - D_b(50)LD}{D_b(50)IA}$
775	27.5	7	MIBC	805	790	1.86
900	17.0	9	MIBC	538	518	3.72
1200	38.0	9	MIBC	437	407	6.86
1050	27.5	7	A65	369	311	15.72
1200	17.0	5	A66	292	187	35.96

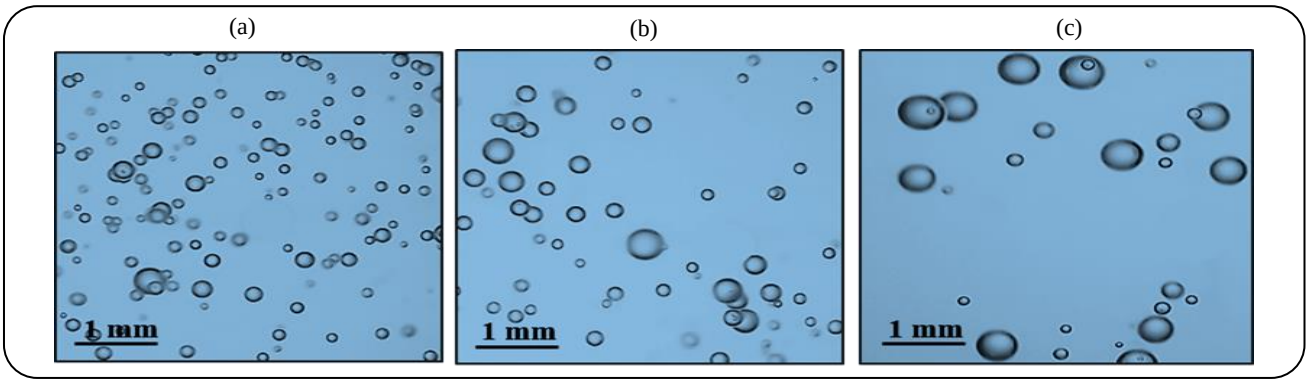

Fig. 13: The image of bubbles at different impeller speeds, a) 1200 RPM, b) 900 RPM, c) 700 RPM.

Comparison between the LD and IA

In order to validate the accuracy of the LD bubble size measurement as a direct method, the results of LD and IA were compared in the same conditions. To see the possible variations in the measurement, the size of bubbles is measured in different experiments (Table. 1) by these two methods. The difference between the LD and IA results is significant when $D_b(50)$ is in the range of -400+200µm. These differences could be explained by the fact that in the IA measurement, bubbles move vertically in a longer distance during taking samples and before imaging. Therefore, the bubbles have a higher possibility to coalesce in the IA in comparison with the LD measurement. On the other hand, in LD measurement setup, bubbles move in a horizontal and shorter path toward the LPSA. In addition, it seems that bubble coalescence happens more in the image analysis method due to its longer measurement time.

Comparing IA with LD revealed that IA is not as efficient as LD while the bubble size range is less than 200 µm, due to the long process of IA and failure to detect these bubbles. It is reported that IA is mostly suitable for the determination of bubbles which are larger than 200 µm [30, 50, 51]. In other words, direct LD measurement can provide more accurate information about the size of fine bubbles.

The comparison of IA and LD methods is performed in a liquid-gas system. According to the table above, the difference between the two measurement methods is less than 7% (6.86%) in the size range of +400-800 microns. However, with the bubble size reduction to 200 microns, the difference between the two methods has increased up to 36%. Also, the results show that the Db(50) of the bubbles is always larger by the IA method than that by the LD method under the same experimental conditions.

The advantages of the LD, including the easy, high speed, and wide range of bubble size measurement introduce this technique as an attractive alternative to the IA for the rapid measurement of bubble size in the mechanical flotation cells.

CONCLUSIONS

The direct measurement of bubbles size distribution in a mechanical laboratory flotation cell under various conditions was assessed using the reliable laboratory-scale Laser Diffraction (LD) method. Image Analysis (IA) as another direct method was considered for comparison purposes. To assess the capability of LD for the bubble size measurement in different conditions, effective parameters on bubble size (frother type, aeration rate, pH value, temperature, and impeller speed) were employed in different

values to generate various bubble sizes. According to the results, the bubbles' sizes measured by the two methods were in very good agreement in the size range of +400-800 microns. IA and LD results difference was less than 7% in this size range. Results also indicated that as the size of the bubbles decreased, the difference in the two methods of measurement increased. Since the size range of the bubbles in the mechanical flotation cells is about +600–2000 microns, the LD method achieves a high accuracy of measurement.

Received : Mar. 11, 2020 ; Accepted : June 15, 2020

REFERENCES

[1] Bailey M.E., "Analysis of Bubble Size Distributions Using the McGill Bubble Size Analyser.", MSc. Thesis, McGill University, Montreal, Canada (2004).

[2] Besagni, G., Inzoli. F., Ziegenhein, T. Two-Phase Bubble Column: A Comprehensive Review, *ChemEngineering* , **2(2):**13-(2018).

[3] Ahmed N., Jameson G.J., The Effect of Bubble Size on the Rate of Flotation of Fine Particles, *Int J. of Min. Proc.*, **14**: 195–215 (1985).

[4] Yoon R.H., Luttrell G.H., The Effect of Bubble Size on Fine Particle Flotation, *Minerals Processing and Extractive Metallurgy Review*, **5**: 101–122 (1989).

[5] Gorain B.K., Franzidis J.P., Manlapig E.V., Studies on Impeller Type, Impeller Speed and Air Flow Rate in An Industrial Scale Flotation Cell .4. Effect of Bubble Surface Area Flux on Flotation Performance, *Minerals Engineering*, **10(4)**: 367-379 (1997).

[6] Kamali Moaveni A., Design, Construction, and Performance Test of a Laboratory Column Flotation Apparatus, Montan University (2015).

[7] Prakash R., Majumder S.K., Singh A., Flotation Technique: Its Mechanisms and Design Parameters, *Chemical Engineering and Processing*, **127**: 249-270 (2018).

[8] Jung S.Y., Park H.W., LEE S.J., Simultaneous Measurement of Bubble Size, Velocity and Void Fraction In Two-Phase Bubbly Flows with Time-Resolved X-Ray Imaging, *Journal of Synchrotron Radiation*, **21**: 424-429 (2014).

[9] Thomas B.G., Dennisov A., Bai H., "Behavior of Argon Bubbles During Continuous Casting of Steel", *The Proceeding of 80th Steelmaking Conference*, 13-16, Chicago (1997).

[10] Nikhita B., Deekshith P., Guguluto S. K., A Review of Methodologies to Determine Bubble Diameter and Bubble Velocity, *International Journal of Scientific and Research Publications*, **2**: 2250-3153 (2012).

[11] Pandit A.B., Varley J., Thrope R.B., Davidson J.F., Measurement of Bubble Size Distribution - An Acoustic Technique, *Chemical Engineering Science*, **47**: 1079-1089 (1992).

[12] Ksentini I., Kotti M., Ben Mansour L., Effect of Liquid Phase Physicochemical Characteristics on Hydrodynamics of an Electroflotation Column, *Desalination and Water Treatment*, 800279, 1-8, (2013)

[13] Nesset J.E., Hernandez-Aguilar J.R., Acuna C., Gomez C.O., Finch J.A., Some Gas Dispersion Characteristics of Mechanical Flotation Machines, *Minerals Engineering*, **19**: 807–815 (2006).

[14] Hernandez-Aguilar J.R., Gomez C.O., Finch J.A., A Technique for the Direct Measurement of Bubble Size Distributions in Industrial Flotation Cells, Proceedings of the 34th Annual Meeting of the Canadian Mineral Processors, 389-402 (2002).

[15] Rodrigues R.T., Rubio J., New basis for Measuring the Size Distribution of Bubbles, *Minerals Engineering*, **16(8)**: 757-765 (2003).

[16] Xu R., Particle Characterization: Light Scattering Methods, Particle Technology Series, Chap. 3., (2002).

[17] ISO 13320-1, 1999(E). Particle Size Analysis- Laser Diffraction Methods, Part 1, General Principals.

[18] Couto H.J.B., Melo M.V., Massarami G., Treatment of Milk Industry Effluent by Dissolved Air Flotation, *Brazilian Journal of Chemical Engineering*, **21**: 83-91 (2004).

[19] Hudson J.B., Couto, Danial G. N., Reiner N., Silvia C.A., Micro-Bubble Size Distribution Measurements by Laser Diffraction Technique, *Minerals Engineering*, **22**: 330-335 (2008).

[20] "Particle Size Analysis-Laser Diffraction Methods, BS ISO 13320:2009".

[21] Azgomi F., "Characterizing Frothers by Their Bubble Size Control Properties", MSc. Thesis, McGill University, Montreal, Canada (2006).

[22] Moyo P., "Characterization of Frothers by Water Carrying Rate", Ph.D. Thesis, McGill University, Montreal, Canada (2005).

[23] Finch J.A., Gelinas S., Moyo P., Frother-Related Research at McGill University, *Minerals Engineering*, **19**: 726–733 (2006).

[24] Khoshdast H., Sam A., Flotation Frothers: Review of Their Classifications, Properties and Preparation, *The Open Mineral Processing Journal*, **4**: 25-44 (2011).

[25] Przemyslaw B.K., Determination of Critical Coalescence Concentration and Bubble Size for Surfactants Used as Flotation Frothers, *Industrial & Engineering Chemistry Research*, **52**: 11752 −11757 (2013).

[26] Zhang W., Nesset J.E., Rao R.., Finch J.A., Characterizing Frothers Through Critical Coalescence Concentration (CCC) 95-Hydrophile-Lipophile Balance (HLB) Relationship, *Minerals*, **2**: 208−227 (2012).

[27] Nesset J.E., Finch J.A., Gomez C.O., "Operating Variables Affecting Bubble Size in Force-Air Mechanical Flotation Machines", *Proceeding of the 9th Mill Operators Conference*, Fremantle, Australia, March 19–21, (2007).

[28] Dobby G.S., Finch J.A., Particle Collection in Columns- Gas Rate and Bubble Size Effects, *Canadian Metallurgical Quarterly*, **25**: 9-13 (1986).

[29] Gupta A.K., Banerjee P.K., Mishra A., Satish P., Effect of Alcohol and Polyglycol Ether Frothers on Foam Stability, Bubble Size and Coal Flotation, *International Journal of Mineral Processing*, **82**: 126– 37 (2007).

[30] Shahbazi B., Rezaei B., The Effect of Type and Dosage of Frothers on Coarse Particles Flotation, *Iranian Journal of Chemistry and Chemical Engineering (IJCCE)*, **28(1)**: 95-101 (2009).

[31] Jin F., Li J., Ye X., Wu Ch., Effects of pH and Ionic Strength on the Stability of Nanobubbles in Aqueous Solutions of R-Cyclodextrin, *Journal of Physical Chemistry B*, **111**: 11745-11749 (2007).

[32] Elmashdy A.M., Mirnezami M., Finch J.A., Zeta Potential of Air Bubbles in Presence of Frothers, *International Journal of Mineral Processing*, **89**: 40–43 (2008).

[33] Wu Ch., Nesset K., Masliyah J., Xu Z., Generation and Characterization of Submicron Size Bubbles, *Advances in Colloid and Interface Science*, 123–132 (2012).

[34] Jin, F., Li, J., Ye, X., Wu, Ch. Effects of pH and Ionic Strength on the Stability of Nanobubbles in Aqueous Solutions of r-Cyclodextrin, *J. Phys. Chem. B*, **111**: 11745-11749 (2007).

[35] Phan Ch.M., Nakahara H., Shibata O., Moroi Y., Le T.N., Ang H.M. 'Surface Potential of Methyl Isobutyl Carbinol Adsorption Layer at the Air/Water Interface, *The Journal of Physical Chemistry*, **116**: 980–986 (2012).

[36] Zhang W., Nesset J.E., Finch J.A., Bubble Size as a Function of Some Situational Variables in Mechanical Flotation Machines, *Journal of Central South University*, **21**: 720−727 (2014).

[37] Wang L.K., Shammas N.K., Selke W.A., Aulenbach D.B., "Gas Dissolution, Release, and Bubble Formation in Flotation Systems, Handbook of Environmental Engineering", Volume 12: Flotation Technology (2010).

[38] Najafi A., Drelich J., Yeung A., Xu Z., Masliyah J., A Novel Method of Measuring Electrophoretic Mobility of Gas Bubbles, *Journal of Colloid and Interface Science*, **308**: 344–350 (2007).

[39] Ahmadi R., "Flotation of Fine Particles from Mine Tailings by Coalescent of Nano-microbubbles", Ph.D. Thesis, Tarbiat Modares University, Tehran, Iran.

[40] Zhang X. H., Li G., Wu Z.H., Zhang X. D., Hu J., Effect of Temperature on the Morphology of Nanobubbles at Mica/Water Interface, *Chinese Physics*, **14(9)**: 1774-05 (2005).

[41] Seguineau De Preval E., Fabrice D., Gilles M., Gérard C., Samir M., Influence of Surface Properties and Bulk Viscosity on Bubble Sizeprediction During Foaming Operation, *Colloids and Surfaces A: Physicochem. Eng. Aspects*, **442**: 88–97 (2014).

[42] Gorain B.K., Franzidis J.P., Manlapig E.V., Studies on Impeller Type, Impeller Speed and Air Flow Rate in an Industrial Scale Flotation Cell. Part 4: Effect of Bubble Surface Area Flux on Flotation Performance, *Minerals Engineering*, **10**: 367–379 (1997).

[43] Miskovic S., "An Investigation of the Gas Dispersion Properties of Mechanical Flotation Cells: An In-Situ Approach", Ph.D. Thesis, Virginia Polytechnic Institute and State University, Blacksburg, Virginia (2011).

[44] Yang X., Aldrich CH., Effects of Impeller Speed and Aeration Rate on Flotation Performance of Sulphide Ore, *Transactions of Nonferrous Metals Society of China*, **16**: 185-190 (2005).

[45] Javor Z., Schreithofer N., Heiskanen K., Kernel Functions to Flotation Bubble Size Distributions, *Minerals Engineering*, **125**: 200-205 (2018).

[46] Mesa D., Morrison A.J., Brito-Parada P.R., "Effect of Impeller Design on Bubble Size and Froth Stability", *International Mineral Processing Congress (IMPC)*, Moscow, September 16-21 (2018).

[47] Sawyerr F., Deglon D.A., O'connor C.T., Prediction of Bubble Size Distribution In mechanical Flotation Cells, *The Journal of The South African Institute of Mining and Metallurgy*, **98(45)**: 179-185 (1998).

[48] Gorain, B.K., Franzidis, J.P., Manlapig, E.V., The Empirical Prediction of Bubble Surface Area Flux in Mechanical Flotation Cells From Cell Design and Operation Data, *Minerals Engineering*, **12**: 309-322 (1999).

[49] Grau R.A., Heiskanen K., Bubble Size Distribution in Laboratory Scale Flotation Cells, *Minerals Engineering*, **18**: 1164–1172 (2005).

[50] Azgomi F., Gomez C.O., Finch J.A., Correspondence of Gas Holdup and Bubble Size in Presence of Different Frothers, *International Journal of Mineral Processing*, **83**: 1–11 (2007)

[51] Finch J.A., Nesset J., Acuna C., Role of Frother on Bubble Production and Behaviour in Flotation, *Minerals Engineering*, **21**: 949−957 (2008).